

# Mutational analysis of the carbohydrate binding activity of the tobacco lectin

Dieter Schouppe · Pierre Rougé · Yi Lasanajak ·  
Annick Barre · David F. Smith · Paul Proost ·  
Els J. M. Van Damme

Received: 1 June 2010 / Revised: 20 July 2010 / Accepted: 23 July 2010 / Published online: 19 August 2010  
© Springer Science+Business Media, LLC 2010

**Abstract** At present the three-dimensional structure of the tobacco lectin, further referred to as Nictaba, and its carbohydrate-binding site are unresolved. In this paper, we propose a three-dimensional model for the Nictaba domain based on the homology between Nictaba and the carbohydrate-binding module 22 of *Clostridium thermocellum* Xyn10B. The suggested model nicely fits with results from circular dichroism experiments, indicating that Nictaba consists mainly of  $\beta$ -sheet. In addition, the previously identified nuclear localization signal is located at the top of the protein as a part of a protruding loop. Judging from this model and sequence alignments with closely related proteins, conserved glutamic acid and tryptophan residues in the Nictaba sequence were selected for mutational analysis. The mutant DNA sequences as well as the original Nictaba

sequence have been expressed in *Pichia pastoris* and the recombinant proteins were purified from the culture medium. Subsequently, the recombinant proteins were characterized and their carbohydrate binding properties analyzed with glycan array technology. It was shown that mutation of glutamic acid residues in the C-terminal half of the protein did not alter the carbohydrate-binding activity of the lectin. In contrast, mutation of tryptophan residues in the N-terminal half of the Nictaba domain resulted in a complete loss of carbohydrate binding activity. These results suggest that tryptophan residues play an important role in the carbohydrate binding site of Nictaba.

**Keywords** *Nicotiana tabacum* · Lectin · Carbohydrate-binding · Structure · Mutant

D. Schouppe · E. J. M. Van Damme (✉)  
Department of Molecular Biotechnology,  
Laboratory of Biochemistry and Glycobiology, Ghent University,  
Coupure Links 653,  
9000 Ghent, Belgium  
e-mail: ElsJM.VanDamme@UGent.be

P. Rougé · A. Barre  
Surfaces Cellulaires et Signalisation chez les Végétaux,  
UMR-CNRS 5546, Pôle de Biotechnologie Végétale,  
Toulouse, France

Y. Lasanajak · D. F. Smith  
Department of Biochemistry,  
Emory University School of Medicine,  
Atlanta, GA 30322, USA

P. Proost  
Laboratory of Molecular Immunology,  
Rega Institute for Medical Research, University of Leuven,  
Minderbroedersstraat 10,  
3000 Leuven, Belgium

## Introduction

Lectins are defined as proteins that can bind to carbohydrate structures in a reversible and non-catalytic way [1]. So far about 500 lectins from plants have been purified and characterized to some extent. Based on their three-dimensional structure and sequence, all plant lectins can be classified into 12 distinct lectin families each typified by a specific lectin domain [2, 3].

Historically, the first plant lectins discovered were purified from tissues in which they are present in high concentrations. It was shown that most of these lectins locate to the vacuole of the plant cell. Because of their high abundance and the ease of purification with affinity chromatography techniques, these “vacuolar” plant lectins were the favorite proteins for many structural biologists. Hence, a significant amount of structural information on these vacuolar lectins and their interaction with carbohy-

drate ligands is available [4, 5]. It is now believed that these proteins act as defense and/or storage proteins in plants [2].

In the past decade, several new lectins have been discovered that reside in the nucleocytoplasmic compartment of the plant cell [3]. Typically these lectins are present in very low concentrations and are often inducible by stress factors such as salt, drought or pathogen attack. It is believed that these nucleocytoplasmic lectins fulfill a role in the stress physiology of the plant cell. Although nucleocytoplasmic lectins have been found in at least six lectin families, no information is available yet regarding their three-dimensional structure and the conformation of their glycan binding sites.

The *Nicotiana tabacum* agglutinin, abbreviated as Nictaba, was first reported in 2002 when it was purified from tobacco leaves treated with jasmonates [6]. Biochemical analysis showed that Nictaba exists as a dimer of two unglycosylated 19 kDa subunits. Molecular cloning of the coding sequence revealed that Nictaba shares more than 40% sequence similarity with a group of carbohydrate-binding proteins known as the Cucurbitaceae phloem lectins. A more extensive database search revealed that the Nictaba sequence is widespread in plants belonging to different taxonomic groups. In some cases the Nictaba sequence is present as a single domain, while in other cases it is part of a larger fusion protein [7]. Therefore, Nictaba can be considered as a representative for the (carbohydrate binding) domain present in the family of so-called Nictaba-related proteins [8].

Using immuno-fluorescence microscopy with a polyclonal antibody directed against Nictaba, it was shown that the localization of this lectin is confined to the nucleus and the cytoplasm of leaf parenchym cells [6]. This nucleocytoplasmic localization was confirmed by confocal microscopy of an EGFP-Nictaba fusion protein. In addition, it was demonstrated that the basic tetrapeptide (102-LysLysLysLys-105) is required and sufficient for transport of Nictaba from the cytoplasm into the nucleus [9]. Hapten inhibition assays using mono- and oligosaccharides revealed that Nictaba exhibits affinity towards  $\beta$ -,4 linked GlcNAc oligomers. With the advent of glycan array technology, it could be demonstrated that Nictaba also shows affinity for high mannose and complex type N-glycans, suggesting that the binding site of Nictaba is most complementary to the core GlcNAc<sub>2</sub>Man<sub>3</sub> structure [9].

The expression level for Nictaba in tobacco leaves is very low, even after treatment of the plant with jasmonates or insect herbivory [10, 11]. Consequently, the purification of Nictaba starting from tobacco leaves is very inefficient. Moreover, Nictaba preparations purified from tobacco leaf material often contain low molecular weight impurities, even after several affinity chromatography purification steps. Since these contaminants—most probably phenolic compounds—hamper the crystallization of the lectin, the

three-dimensional structure of Nictaba could not be resolved yet. To overcome some of these problems, Nictaba has been expressed in the methylotrophic yeast *Pichia pastoris* [12]. Nictaba was purified from the cell pellet and the culture medium of *Pichia* strain GS115 using a combination of anion exchange chromatography and affinity chromatography on a column with immobilized ovomucoid. It was shown that the purified recombinant Nictaba exhibited similar biochemical properties and carbohydrate binding specificity, compared to native Nictaba from tobacco [12].

Due to the lack of information related to the three-dimensional structure of Nictaba, little is also known about the carbohydrate-binding site of the lectin. In an attempt to unravel which amino acids are important for carbohydrate-binding activity of the protein, a three-dimensional structure model of Nictaba was made based on the homology between Nictaba and the carbohydrate-binding module 22 of *Clostridium thermocellum* Xyn10B. Judging from this model and sequence alignments with closely related proteins, conserved glutamic acid and tryptophan residues in the Nictaba sequence were selected for mutational analysis. The mutant sequences as well as the original Nictaba sequence were expressed in *Pichia pastoris*. After purification, carbohydrate binding properties of the mutant proteins were analyzed with glycan array technology and compared to the carbohydrate binding properties of Nictaba.

## Materials and methods

### Hydrophobic cluster analysis

Multiple amino acid sequence alignments were carried out with CLUSTAL-X [13] using the Risler's structural matrix for homologous amino acid residues [14]. Hydrophobic Cluster Analysis (HCA) [15] was performed to delineate the structurally conserved strands of  $\beta$ -sheets along the amino acid sequence of Nictaba using the carbohydrate-binding module 22 of *Clostridium thermocellum* Xyn10B [16] as a model. HCA plots were generated using the HCA server (<http://bioserv.rpbs.jussieu.fr>).

### Molecular modeling

Molecular modeling of Nictaba was carried out on a Silicon Graphics O2 R10000 workstation, using the programs InsightII, Homology and Discover3 (Accelrys, San Diego CA, USA). The atomic coordinates of the *Clostridium thermocellum* Xyn10B carbohydrate-binding module [4] (RCSB Protein Data Bank code 1H6X) were used to build the three-dimensional model of the lectin. Although

Nictaba shares low percentages of identity (~14%) and similarity (56%) with the carbohydrate binding domain of *C. thermocellum*, HCA suggested a very similar structure for both proteins (result not shown). Steric conflicts were corrected during the model building procedure using the rotamer library [17] and the search algorithm of the Homology program [18] to maintain proper side-chain orientation. An energy minimization of the final model was carried out by 200 cycles of steepest descent using the cvff forcefield of Discover. PROCHECK [19] was used to assess the geometric quality of the three-dimensional model. In this respect, about 80% of the residues of Nictaba were correctly assigned to the best allowed regions of the Ramachandran plot, the remaining residues being located in the generously allowed regions of the plot except for five residues (Asp17, Gln20, Val33, Trp41, Leu116), which occur in the non allowed region (result not shown). Electrostatic potentials were calculated and displayed with GRASP using the parse3 parameters [20]. The solvent probe radius used for molecular surfaces was 1.4 Å and a standard 2.0 Å-Stern layer was used to exclude ions from the molecular surface [21]. The inner and outer dielectric constants applied to the protein and the solvent were fixed at 4.0 and 80.0, respectively, and the calculations were performed keeping a salt concentration of 0.145 M. Ribbon diagram and molecular surface of Nictaba were drawn with PyMol (W. L. DeLano (<http://pymol.sourceforge.net>)).

## Bioinformatics analyses

Nictaba domains were identified by performing a pBLAST search against the non-redundant protein sequences database (<http://blast.ncbi.nlm.nih.gov/Blast.cgi>). Multiple sequence analysis was carried out using the ClustalW2 sequence analysis tool (<http://www.ebi.ac.uk/>).

## Expression of Nictaba sequences in *Pichia pastoris*

Cloning and expression of native and mutant forms of Nictaba was performed using the EasySelect *Pichia* Expression Kit from Invitrogen (Carlsbad, CA USA). The coding sequence for Nictaba was amplified by PCR from a pUC plasmid (Genbank accession number AF389848, [6]) using primers evd 65 and evd 66. The Nictaba coding sequence was mutated using overlap PCR with primer sequences shown in Table 1. PCR was carried out using the Phusion polymerase with proof reading activity (New England Biolabs, Ipswich, MA USA). All Nictaba sequences were amplified using 5' and 3' primers with XbaI and EcoRI overhangs, respectively, to allow cloning in the pPICZαA vector (EasySelect *Pichia* expression kit, Invitrogen) that was cut with the same restriction enzymes. The ligated DNA was heat shock transformed in Top10F' cells and transformants were selected on LB agar plates containing 0.25 µg/ml zeocin (Invitrogen). Plasmid DNA was purified using the E.Z.N.A.® Plasmid Mini Kit (Omega Bio-Tek,

**Table 1** List of primer sequences used to amplify the original and mutant forms of Nictaba

Primer	Properties	Sequence (5'-3')
Native Nictaba		
Evd 65	Forward	cag tgg ata gcc gca aga gac ctt tc
Evd 66	Reverse	tta gtt tgg acg aat gtc gaa gcc c
Nictaba mutant 1		
Evd 12	5' EcoRI	ggc gga gaa ttc acc atg caa ggc cag tgg ata gcc gc
Evd 303	Reverse: E128→A128/E135→A135	att gat tgc cat caa cct cat ttc gac tgc acc atc ctc
Evd 302	Forward: E128→A128/E135→A135	aga gga tgg tgc agt cga aat gag gtt gat ggc aat caa t
Evd 315	3' XbaI	ccc gct ttc tag aca gtt tgg acg aat gtc gaa gcc
Nictaba mutant 2/3		
Evd 376	5' EcoRI	gaa ttc acc atg caa ggc cag tgg ata
Evd 377	Reverse	
	Mutant 2: W22→L22;W15→L15	tgt caa gta ctg agg att gtc cac caa tgt
	Mutant 3: W15→L15	tgt caa gta ctg agg att gtc cac cca tgt
Evd 378	Forward	
	Mutant 2: W15→L15;W22→L22	aca ttg gtg gac aat cct cag tac ttg aca
	Mutant 3: W15→L15	aca ttg gtg gac aat cct cag tac tgg aca
Evd 379	3' XbaI	tct aga cag ttt gga cga atg tcg aag

Norcross, GA USA). Proper insert orientation and sequence of Nictaba and its mutant forms was verified by sequencing using 5' and 3' AOX1 specific primers evd 21 (5' GACTGGTTCCAATTGACAAGC3') and evd 22 (5' GCAAATGGCATTCTGACATCC3') (carried out by LGC Genomics GmbH, Berlin, Germany). The plasmid DNA was linearized with the restriction enzyme SacI (Fermentas, St. Leon-Rot, Germany) and purified before transformation of *Pichia*. *Pichia pastoris* strains GS115 (Mut<sup>+</sup> His<sup>−</sup>—Nictaba mutant 1 and recombinant Nictaba) and KM71H (Mut<sup>S</sup> His<sup>+</sup>Arg<sup>+</sup>—Nictaba mutant 2, 3) were electroporated with 5 µg of linearized DNA using a GenePulser® (Bio-Rad, Hercules, CA USA) with pulse settings of 25 µF, 1.5 kV and 200Ω, and spread on YPDS plates (1% yeast extract, 2% peptone, 2% dextrose, 2% sorbitol, 2% agar, 100 µg/ml zeocin (Invitrogen)). Selected colonies were grown overnight in 5 ml BMGY medium (1% yeast extract, 2% peptone, 100 mM potassium phosphate, pH 6.0, 1.34% YNB, 4×10<sup>−5</sup>% biotin, 1% glycerol) at 30°C in a shaker incubator at 250 rpm. The next day, cultures were washed with water, resuspended in BMMY medium (1% yeast extract, 2% peptone, 100 mM potassium phosphate, pH 6.0, 1.34% YNB, 4×10<sup>−5</sup>% biotin, 0.5% methanol) and grown for 4 days. Every day, methanol was added to a final concentration of 2%. After 4 days, protein profiles in medium and cell pellet were compared. Proteins were precipitated from the medium with 10% TCA. Protein extraction from the pellet was done by vortexing with glass beads (108 µm diameter, Sigma, St Louis, MO USA) in 20 mM 1,3 diaminopropane buffer. Protein extracts were analyzed by SDS-PAGE and Western blot analysis.

#### Large scale culture and purification of recombinant proteins

Transformed yeast colonies were grown overnight in 5 ml BMGY (30°C, 250 rpm). The next day, cultures were transferred to 100 ml BMGY in 250 ml erlenmeyer flasks and allowed to grow until an OD<sub>600</sub> of 2–6 was reached. Cells were washed with water, and transferred to 200 ml BMMY in 1 l Erlenmeyer flasks. Methanol was added to a final concentration of 2% every 24 h. After 72 h, the medium was collected by centrifugation and proteins were precipitated overnight with 80% ammonium sulphate. In the case of Nictaba mutant 1, precipitated proteins were resuspended in a small volume of 20 mM diaminopropane and dialysed against the same buffer overnight with several buffer changes. Subsequently, the sample was loaded on a Q Sepharose Fast Flow column (Ø 15 mm, height 4 cm, GE healthcare, Uppsala, Sweden) previously equilibrated with 20 mM diaminopropane. After extensive washing with diaminopropane until OD<sub>280</sub><0.3, bound proteins were

eluted with 20 mM Tris pH 8.7 containing 0.5 M NaCl. The most concentrated protein fractions from the anion exchange column were pooled and loaded on a gel filtration column (Sephacryl S-100, Ø 2 cm, height 60 cm, GE healthcare). For Nictaba mutants 2 and 3, ammonium sulphate precipitated proteins were resuspended in 20 mM diaminopropane and directly separated on the gel filtration column. Fractions from the gel filtration column were collected and analyzed by SDS-PAGE and Western Blot analysis.

#### Glycan array screening

The microarrays are printed as described previously [22]. The analyses reported here were performed on Mammalian Printed Array Version 3.0 for the Nictaba mutant 1 and Version 4.0/4.1 for all other proteins (see <https://www.functionalglycomics.org/static/consortium/resources/resourcecoreh8.shtml>). Recombinant Nictaba (original or mutant forms) purified from *Pichia pastoris* was labeled using the Alexa Fluor® 488 Protein Labeling Kit from Invitrogen following the manufacturer's instructions. The labeled proteins were applied to separate microarray slides and incubated under a cover slip for 60 min in a dark, humidified chamber at room temperature. After incubation, the cover slips are gently removed in a solution of Tris-buffered saline containing 0.05% Tween 20 and washed by gently dipping the slides 4 times in successive washes of Tris-buffered saline containing 0.05% Tween 20, Tris-buffered saline, and deionized water. After the last wash, the slides are spun in a slide centrifuge for approximately 15 sec to dry and are immediately scanned in a PerkinElmer ProScanArray MicroArray Scanner using an excitation wavelength of 488 nm and ImaGene software (BioDiscovery Inc., El Segundo, CA USA) to quantify fluorescence. The data are reported as average Relative Fluorescence Units (RFU) of 4 replicate values after removal of the high and low values of the six replicates of each glycan presented on the array.

#### Amino terminal sequence analysis

Recombinant proteins purified from *Pichia pastoris* were analyzed by SDS-PAGE and electroblotted on a ProBlot™ polyvinylidene difluoride membrane (Applied Biosystems, Foster City, CA USA). The membrane was stained with a 1:1 mix of Coomassie brilliant blue and methanol. The protein of interest was excised from the blot and the N-terminal sequence determined by Edman degradation performed on a model Procise 491cLC protein sequencer without alkylation of cysteines (Applied Biosystems, Foster City, CA USA).



## Analytical methods

The protein content of the samples was estimated using the Coomassie (Bradford) Protein Assay Kit (Thermo Fisher Scientific, Rockford, IL USA), based on the Bradford [23] dye-binding procedure. Extracts from *Pichia* were analyzed for protein expression by SDS-PAGE using 15% polyacrylamide gels under reducing conditions as described by Laemmli [24]. Proteins were visualized by staining with Coomassie Brilliant Blue R-250. For Western blot analysis, samples separated by SDS-PAGE were electrotransferred to 0.45  $\mu$ m polyvinylidene fluoride (PVDF) membranes (Biotrace™ PVDF, PALL, Gelman Laboratory, Ann Arbor, MI USA). After blocking the membrane in Tris-Buffered Saline (TBS: 10 mM Tris, 150 mM NaCl, 0.1% (v/v) Triton X-100, pH 7.6) containing 5% (w/v) BSA, blots were incubated for 1 h with a mouse monoclonal anti-His (C-terminal) antibody (Invitrogen), diluted 1/5000 in TBS. The secondary antibody was a 1/1000 diluted rabbit anti-mouse IgG labeled with horse radish peroxidase (Dako Cytomation, Glostrup, Denmark). Immuno-detection was achieved by a colorimetric assay using 3,3'-diaminobenzidine tetrahydrochloride (Sigma-Aldrich, St. Louis Missouri, MO USA) as a substrate.

## Results

### Three-dimensional model for Nictaba

The three-dimensional model built for Nictaba essentially consists of a  $\beta$ -sandwich structure composed of two  $\beta$ -sheets of four and five antiparallel  $\beta$ -strands, respectively, connected by extended loops (Fig. 1a). The previously identified nuclear localization signal [6] (LysLysLysLys) occurs at the top of a well exposed loop which protrudes in the solvent. Mapping of electrostatic potentials on the molecular surface of Nictaba also revealed an extended electronegatively charged groove that most probably corresponds to the glycan binding site of the lectin (Fig. 1b). Two well exposed glutamic acid residues (Glu138 and Glu145) account for the electronegative character of the groove and—according to the model—could be involved in the binding of the GlcNAc<sub>2</sub>Man<sub>3</sub> oligomer. Interestingly, a  $\beta$ -strand forms a sort of barrier, thus separating an electronegatively charged extension from the central groove. This additional electronegative pocket with two tryptophan residues (Trp15 and Trp22) could contribute to the sugar-binding specificity of Nictaba.

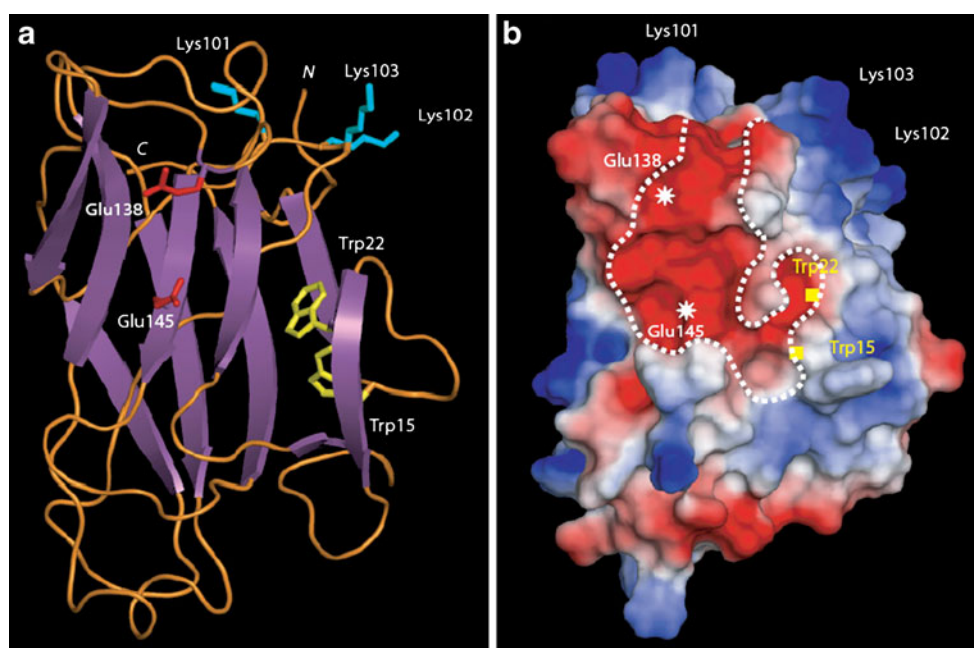


**Fig. 1** Molecular modeling of Nictaba sequence. **a** Ribbon diagram showing the  $\beta$ -sandwich organization of Nictaba. Exposed Lys residues participating to the nuclear localization signal are represented in sticks colored *cyan*. Glu residues occurring at the center of the putative chitin-binding groove are represented in sticks colored *red*. Trp residues possibly participating to the putative carbohydrate-binding pocket are represented in sticks colored *yellow*. N and C

correspond to the N- and C-terminal ends of the polypeptide chain, respectively. **b** Mapping of electrostatic potentials on the molecular surface of the modeled Nictaba. The putative carbohydrate-binding groove is delineated by a dotted white line and the location of important residues is indicated. Electronegatively and electropositively charged areas are colored *red* and *blue*, respectively; neutral regions are shown in *white*

Trp15/22 and Glu138/145 are conserved amino acids in the Nictaba domain

Sequence alignment of the Nictaba domain present in the tobacco leaf lectin and several Nictaba-related proteins from different plant species revealed that Trp15, Trp22 and Glu145 in the Nictaba sequence are strongly conserved in all sequences analyzed (Fig. 2). Although Glu138 is less conserved, the electronegative character of the presumed carbohydrate-binding site is always preserved by the presence of nearby glutamic acid residues.

#### Purification of recombinant proteins from *Pichia pastoris*

To validate the proposed three-dimensional model, a mutational analysis of Nictaba was performed. Mutagenesis of the Nictaba coding sequence was done by overlap PCR. Afterwards, the mutated sequences and the original Nictaba sequence were cloned into a *Pichia pastoris* pPICZαA expression vector. In the sequence of Nictaba mutant 1, Glu138 and Glu145 were mutated into Ala. In the Nictaba mutant 2 Trp15 and Trp22 were changed into Leu, whereas in mutant 3 only Trp15 was modified (Fig. 3a). The resulting constructs were electroporated in *Pichia pastoris* strains GS115 (Nictaba mutant 1 and recombinant Nictaba) or KM71H (Nictaba mutants 2 and 3). Transformed colonies were grown in 1 l cultures and the recombinant proteins purified from the culture medium.

#### Biochemical characterization of recombinant proteins

SDS-PAGE of recombinant proteins purified from *Pichia pastoris* revealed polypeptides with a molecular mass of approximately 22 kDa (Fig. 3a). The size of these polypeptide bands is in good agreement with the molecular mass calculated from the primary sequence taking into account that the recombinant protein contains an additional c-myc epitope and 6×His tag compared to the native Nictaba from tobacco. Further analysis of the purified proteins by Western blot, using a monoclonal antibody directed against the C-terminal polyHis tag (Fig. 3b) and N-terminal sequencing confirmed that the purified proteins correspond to the different Nictaba forms. Edman degradation also showed that the signal peptide of Nictaba mutant 1 was correctly processed at the predicted cleavage site (Fig. 3a). Apart from this form, Nictaba mutant 2 and 3 also exist as slightly smaller proteins, two or four amino acids shorter than the predicted protein (starting at EAEFTMQG or EFTMQGQW). Dynamic light scattering measurements revealed that part of the purified recombinant protein for Nictaba mutants 2 and 3 forms aggregates, making further secondary structure analysis impossible.

#### Carbohydrate-binding specificity of recombinant proteins expressed in *Pichia*

The carbohydrate-binding properties of the recombinant Nictaba proteins (both the original and the mutant forms)

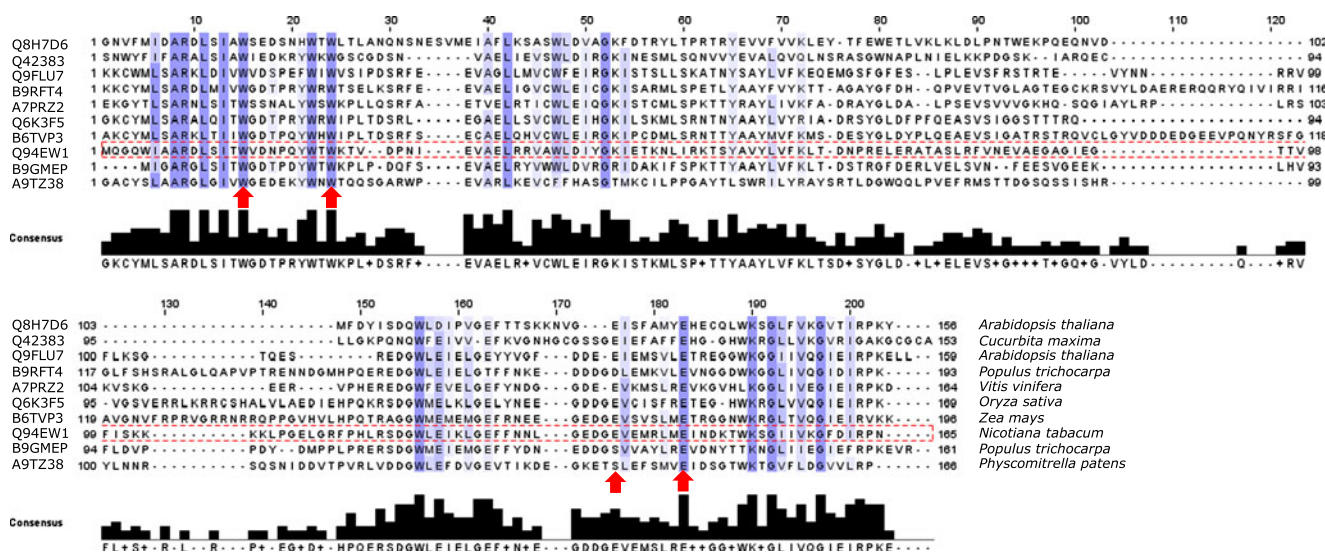


**Fig. 2** Multiple sequence alignment of the amino acid sequences of the Nictaba domain from different plant species. Amino acids that were selected for mutation are indicated by the arrows. The Nictaba sequence is boxed. Accession numbers and species names are indicated in front of the sequence and after the sequence, respectively. Proteins that were aligned are, from top to bottom: hypothetical protein containing a TIR domain from *Arabidopsis thaliana*, dimeric phloem specific lectin PP2

from *Cucurbita maxima*, Nictaba from *Nicotiana tabacum*, F-box family protein from *Populus trichocarpa*, Putative F-box protein PP2-B12 from *Arabidopsis thaliana*, F-box family protein-like from *Oryza sativa*, F-box containing protein from *Vitis vinifera*, putative uncharacterized protein containing a F-Box domain from *Populus trichocarpa*, Phloem-specific lectin from *Zea mays* and predicted protein containing an F-box domain from *Physcomitrella patens*

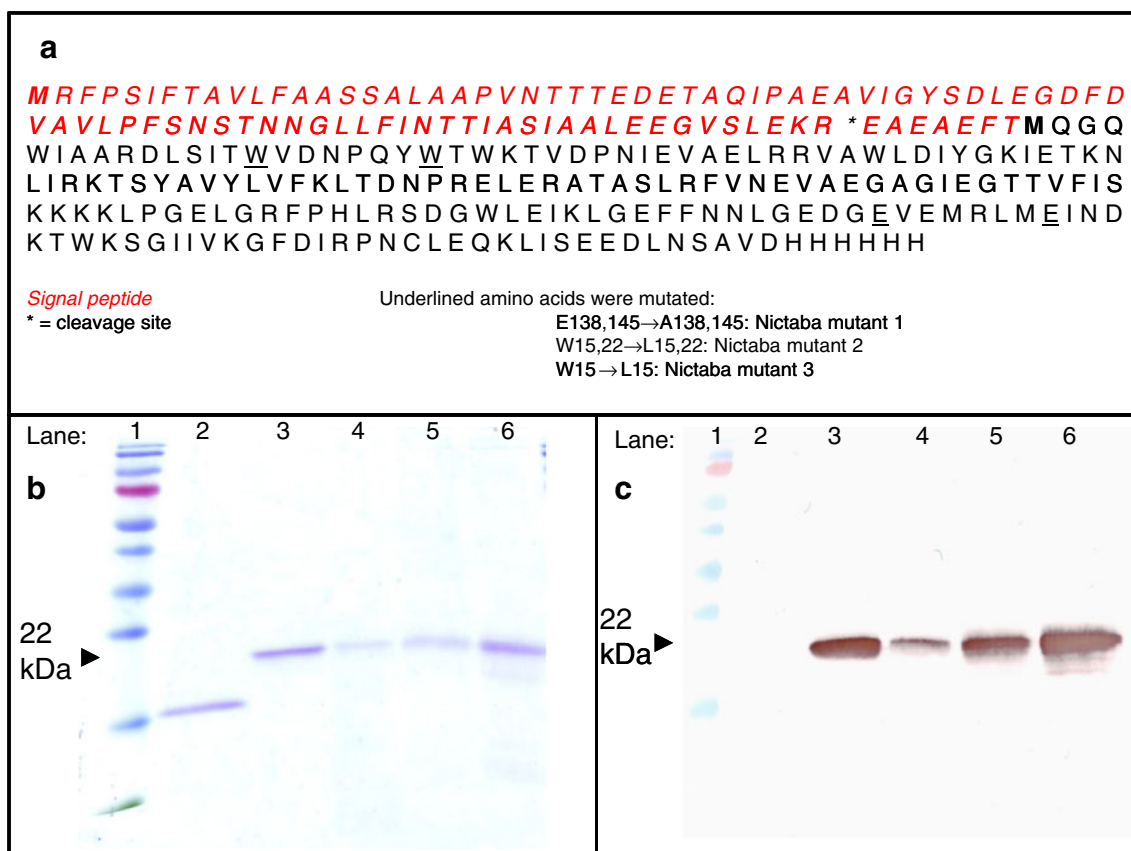


**Fig. 3** Primary sequence of recombinant Nictaba, preceded by an N-terminal signal peptide necessary for secretion and a C-terminal tag containing of a c-myc epitope and a (His)6 tag (**a**). Proteins were analyzed by SDS-PAGE (**b**) and Western blot analysis with a monoclonal anti-His antibody (**c**). Samples are loaded as follows: *lane 1*: molecular weight

marker, *lane 2*: native Nictaba from tobacco; *lane 3*: recombinant Nictaba; *lane 4*: Nictaba mutant 1; *lane 5*: Nictaba mutant 2; *lane 6*: Nictaba mutant 3. Approximately 0.5 µg of each protein was loaded on the gel

were investigated by screening the labeled proteins on a glycan array, and comparison to the sugar-binding specificity of the native Nictaba from tobacco. Analyses of the native tobacco lectin and the recombinant Nictaba expressed in *Pichia* revealed high affinity for complex and high mannose N-type glycans and to a lesser extent for GlcNAc oligomers (Fig. 4a and c). It can thus be concluded that the recombinant Nictaba protein expressed in *Pichia* preserves the carbohydrate binding properties of the native tobacco protein. Mutation of Glu138 and Glu145 in the Nictaba sequence (Nictaba mutant 1) did not significantly change the apparent specificity of the protein for the above-mentioned carbohydrate structures (Fig. 4b). However, mutation of Trp15 and Trp22 (Nictaba mutant 2) drastically altered the carbohydrate-binding properties of the protein and almost completely abolished binding to carbohydrate structures. Similarly, when only Trp22 was changed into a leucine residue (Nictaba mutant 3) no glycan binding could be observed (Fig. 4d). Evidently, the combination of both Glu and both Trp residues in one mutant protein also completely abolished the interaction of this mutant protein with all glycans on the array (data not shown).

A comparative analysis of the glycan array results for native and recombinant Nictaba as well as for Nictaba mutants 1 and 3 was performed. Therefore, all glycan array data were compared by first doing a ranking calculation that “normalizes the values” of different data sets, and assigning a percentile ranking to each RFU. Only the results for the top 25 glycans are shown in Table 2. A detailed analysis of these data demonstrates that the glycan structures with the highest rank for native Nictaba, recombinant Nictaba and Nictaba mutant 1 are very similar and all belong to the high mannose or more complex type N-glycans, whereas the interaction with GlcNAc or GlcNAc oligomers is much weaker.

## Discussion

The tobacco lectin or Nictaba can be regarded as a prototype for a new group of nucleocytoplasmic proteins. Hitherto, the function of the Nictaba domain is unknown and subject to speculation. It is known that Nictaba shares significant sequence similarity with the Cucurbitaceae



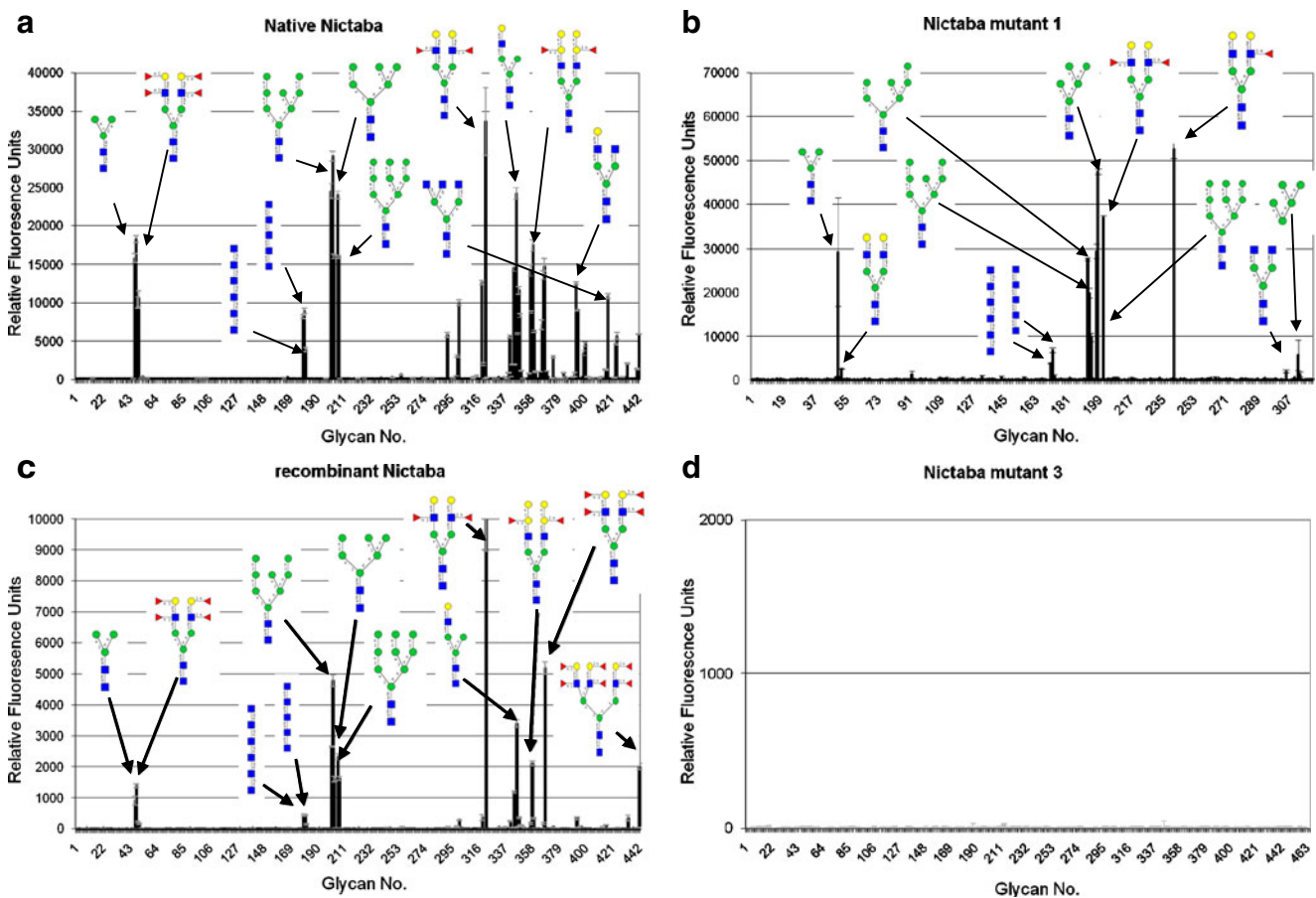


**Fig. 4** Comparative analysis of binding of native Nictaba and recombinant Nictaba proteins purified from *Pichia* on the glycan array. Different panels show interaction of **a**, native Nictaba (150 µg/ml, v4.0); **b**, Nictaba mutant 1 (100 µg/ml, v3.0); **c**, recombinant Nictaba

(210 µg/ml, v4.0); and **d**, Nictaba mutant 3 (200 µg/ml v4.1). The complete primary data set for each protein is available on the website of the Consortium for Functional Glycomics ([www.functionalglycomics.org](http://www.functionalglycomics.org))

phloem lectins (also referred to as PP2 proteins) that are highly conserved within *Cucurbita* species. In these plants, PP2 is one of the most abundant proteins present in the phloem sap. In contrast to Nictaba, PP2 proteins are expressed in the vascular tissue and contain an additional N-terminal peptide as well as a C-terminal domain that is thought to crosslink with the structural P-protein (PP1) through disulfide bridges. The PP2 protein was shown to be secreted into the assimilate stream where it can travel over long distances through the plant and exert its carbohydrate and RNA-binding activities [25]. Extensive database searches with the Nictaba domain signature revealed the existence of Nictaba or PP2-related proteins in a variety of genera belonging to the angiosperms and gymnosperms, of which the latter are known to be devoid of the structural P-protein. In *Arabidopsis*, many Nictaba-like proteins have been identified that have acquired an additional modular N-terminal domain such as an F-box- or TIR-domain. It can therefore be concluded that the Nictaba-domain is widespread in the plant kingdom [8]. It remains to be shown if all these proteins possess carbohydrate-binding activity.

Using hapten inhibition assays and glycan array analyses it was demonstrated that Nictaba exhibits specificity towards  $\beta(1-4)\text{GlcNAc}$  oligomers as well as complex and high mannose N-linked glycans. Because of this dual specificity, it was hypothesized that Nictaba specifically recognizes the  $\text{GlcNAc}_2\text{Man}_3$  core of N-glycan structures. Despite numerous efforts, the three-dimensional structure of Nictaba and its carbohydrate-binding site could not yet be elucidated. Here we present a three-dimensional model of the Nictaba structure based on the structural homology with the carbohydrate-binding module 22 of *Clostridium thermocellum* Xyn10B [16]. According to this model, Nictaba consists of a  $\beta$ -sandwich composed of two  $\beta$ -sheets. Similar to many plant lectins the Nictaba model predicts a structure that consists mainly of  $\beta$ -sheet. These results are in agreement with circular dichroism analyses which revealed that Nictaba consists of 45%  $\beta$ -sheet, 55%  $\beta$ -coil, but no  $\alpha$ -helix [6].

Nictaba contains a typical nuclear localization signal made up of four basic lysine residues. According to the model, this nuclear localization signal is located at the top



**Table 2** Comparative analysis of glycan array results for native and recombinant Nictaba as well as Nictaba mutants 1 and 3

Chart number v4.0	Structure	Native Nictaba		Recombinant Nictaba		Nictaba mutant 1 v3.0		Nictaba mutant 3	
		RFU	Rank <sup>a</sup>	RFU	Rank <sup>a</sup>	RFU	Rank <sup>a</sup>	RFU	Rank <sup>a</sup>
NA	Galβ1-4GlcNAcβ1-2Manα1-3(Fucα1-3(Galβ1-4)GlcNAcβ1-2Manα1-6)Manβ1-4GlcNAcβ1-4GlcNAcβ-Sp20	NA <sup>b</sup>	NA	NA	NA	52664	100	NA	NA
202	Manα1-2Manα1-6(Manα1-3)Manα1-6[Manα1-2Manα1-2Manα1-3]Manβ1-4GlcNAcβ1-4GlcNAcβ-Sp12	32124	100	4775	46	19894	38	1	0
201	Manα1-6[Manα1-2Manα1-3]Manα1-6[Manα1-2Manα1-3]Manβ1-4GlcNAcβ1-4GlcNAcβ-Sp12	30941	96	2651	26	27651	53	6	0
368	Galα1-3Galβ1-4(Fucα1-3)GlcNAcβ1-2Manα1-3(Galα1-3Galβ1-4(Fucα1-3)GlcNAcβ1-2Manα1-6)Manβ1-4GlcNAcβ1-4GlcNAcβ-Sp20	26138	81	5182	50	NA	NA	1	0
322	Fucα1-3(Galβ1-4)GlcNAcβ1-2Manα1-3(Fucα1-3(Galβ1-4)GlcNAcβ1-2Manα1-6)Manβ1-4GlcNAcβ1-4GlcNAcβ-Sp20	25973	81	10296	100	36925	70	−2	0
346	Galβ1-4GlcNAcβ1-2Manα1-3(Manα1-6)Manβ1-4GlcNAcβ1-4GlcNAcβ-Sp12	25012	78	3395	33	NA	NA	3	0
206	Manα1-6(Manα1-3)Manα1-6[Manα1-2Manα1-3]Manβ1-4GlcNAcβ1-4GlcNAcβ-Sp12	23426	73	2321	23	29479	56	1	0
48	Manα1-3(Manα1-6)Manβ1-4GlcNAcβ1-4GlcNAcβ-Sp13	19194	60	1394	14	29183	55	12	0
207	Manα1-6(Manα1-3)Manα1-6(Manα1-3)Manβ1-4GlcNAcβ1-4GlcNAcβ-Sp12	18865	59	1616	16	47537	90	7	0
47	Manα1-3(Manα1-6)Manβ1-4GlcNAcβ1-4GlcNAcβ-Sp12	18598	58	913	9	NA	NA	1	0
319	Galβ1-3GlcNAcβ1-2Manα1-3(Galβ1-3GlcNAcβ1-2Manα1-6)Manβ1-4GlcNAcβ1-4GlcNAcβ-Sp19	16215	50	360	3	124	0	2	0
301	GlcNAcβ1-2Manα1-3(GlcNAcβ1-2Manα1-6)Manβ1-4GlcNAcβ1-4GlcNAcβ-Sp12	15637	49	273	3	2015	4	2	0
359	Galα1-3Galβ1-4GlcNAcβ1-2Manα1-3(Galα1-3Galβ1-4GlcNAcβ1-2Manα1-6)Manβ1-4GlcNAcβ1-4GlcNAcβ-Sp20	15277	48	334	3	NA	NA	6	0
344	Galβ1-4GlcNAcβ1-2Manα1-3Manβ1-4GlcNAcβ1-4GlcNAcβ-Sp12	14927	46	1188	12	NA	NA	3	0
203	Manα1-2Manα1-2Manα1-3(Manα1-2Manα1-3(Manα1-2Manα1-6)Manα1-6)Manβ1-4GlcNAcβ1-4GlcNAcβ-Sp12	14796	46	1605	16	9830	19	2	0
357	Fucα1-2Galβ1-4GlcNAcβ1-2Manα1-3(Fucα1-2Galβ1-4GlcNAcβ1-2Manα1-6)Manβ1-4GlcNAcβ1-4GlcNAcβ-Sp20	14054	44	169	2	NA	NA	4	0
367	Galα1-3(Fucα1-2)Galβ1-4GlcNAcβ1-2Manα1-3(Galα1-3(Fucα1-2)Galβ1-4GlcNAcβ1-2Manα1-6)Manβ1-4GlcNAcβ1-4GlcNAcβ-Sp20	13121	41	168	2	NA	NA	7	0
348	Galβ1-4GlcNAcβ1-2Manα1-3(Galβ1-4GlcNAcβ1-2Manα1-6)Manβ1-4GlcNAcβ1-4(Fucα1-6)GlcNAcβ-Sp22	12978	40	352	3	NA	NA	6	0
180	(GlcNAcβ1-4)5β-Sp8	12695	40	446	4	6910	13	2	0
349	Galβ1-3GlcNAcβ1-2Manα1-3(Galβ1-3GlcNAcβ1-2Manα1-6)Manβ1-4GlcNAcβ1-4(Fucα1-6)GlcNAcβ-Sp22	12408	39	115	1	NA	NA	4	0
393	Galβ1-4GlcNAcβ1-2Manα1-3(GlcNAcβ1-2Manα1-6)Manβ1-4GlcNAcβ1-4GlcNAcβ-Sp12	11677	36	331	3	NA	NA	−1	0
179	(GlcNAcβ1-4)6β-Sp8	11325	35	439	4	3909	7	5	0
50	Galβ1-4GlcNAcβ1-2Manα1-3(Galβ1-4GlcNAcβ1-2Manα1-6)Manβ1-4GlcNAcβ1-4GlcNAcβ-Sp12	10836	34	163	2	2585	5	4	0
442	Fucα1-2Galβ1-4(Fucα1-3)GlcNAcβ1-2(Fucα1-2Galβ1-4(Fucα1-3)GlcNAcβ1-4)Manα1-3(Fucα1-2Galβ1-4(Fucα1-3)GlcNAcβ1-2Manα1-6)Manβ1-4GlcNAcβ1-4GlcNAcβ-N	10726	33	2006	19	NA	NA	1	0
358	Fucα1-2Galβ1-4(Fucα1-3)GlcNAcβ1-2Manα1-3(Fucα1-2Galβ1-4(Fucα1-3)GlcNAcβ1-2Manα1-6)Manβ1-4GlcNAcβ1-4GlcNAcβ-Sp20	10151	32	2110	20	NA	NA	1	0

<sup>a</sup> Percentile ranking: The glycan with the highest RFU is assigned a value of 100<sup>b</sup> NA means that the glycan was not available in that assay; *i.e.*, present on version 4 but not version 3, or present on version 3 and not on version 4

of the protein as part of a protruding loop. It is therefore nicely exposed and can be readily recognized by an import protein that can facilitate transport of the lectin into the nucleus through the nuclear pore protein complex. The Nictaba model also shows the presence of a large electro-negatively charged pocket. A  $\beta$ -strand separates the large central groove from a smaller electro-negatively charged extension. The electro-negative character of the central pocket is mainly due to the presence of several glutamic acid residues, of which Glu138 and Glu145 stand out most prominently. From the second, smaller pocket, two tryptophan residues (Trp15, Trp22) protrude. As commonly observed in many other carbohydrate-binding sites of plant lectins, the conserved tryptophan residues would complete the interaction with the sugar by an aromatic stacking with the pyranose ring of the H-bound sugar. This hypothesis is corroborated by research on other Nictaba-like proteins from the Cucurbitales. Studies of the carbohydrate binding specificity of the Nictaba-like *Luffa acutangula* lectin strongly suggest a role for a tryptophan residue in the carbohydrate binding site, since fluorescence in the near UV-CD spectrum changes upon interaction with its ligand [26, 27]. In addition, thermodynamic studies and fluorescence analysis of the *Coccinia indica* agglutinin with a labeled chito-oligomer of variable length also suggest involvement of a tryptophan residue in the binding site [28]. These results are enforced by chemical modification experiments. However, these results are in sharp contrast with recent findings on the *Cucurbita maxima* phloem exudate lectin. For this lectin it was shown that tryptophan residues are only partially exposed to the aqueous environment and are probably not involved in ligand interaction, because binding of GlcNAc oligomers—which are specifically recognized by the lectin—did not significantly alter the quenching pattern [29].

To validate our proposed three-dimensional model, the Nictaba coding sequence was mutated and recombinant proteins were expressed in and purified from *Pichia pastoris*. Residues Glu138 and Glu148 have been mutated to alanine residues whereas Trp15 and Trp22 have been changed into leucine. The carbohydrate binding properties of these mutant proteins were investigated using the glycan array technology. It was shown that mutation of both designated glutamic acid residues (Nictaba mutant 1) did not influence the carbohydrate binding specificity. Possibly, this could be explained by the presence of other glutamic acid residues nearby, thus preserving the electro-negative character of the binding site. In contrast, mutation of the two tryptophan residues (Nictaba mutant 2) located in a smaller extension of the proposed binding pocket, led to a complete loss of binding of the protein to any of the carbohydrate structures present on the array. Similarly, when only Trp15 was mutated to leucine (Nictaba mutant

3), again no carbohydrate binding was observed, suggesting a complete loss of lectin activity. These results strongly endorse the three-dimensional structure of Nictaba as proposed in the model. We suggest that carbohydrate binding activity of the Nictaba domain is mediated through the large electro-negatively charged groove and hypothesize that hydrophobic interactions between the indole group of Trp15 and the pyranose groups of the glycan molecule stabilize the interactions in the lectin binding site.

**Acknowledgments** This work was funded primarily by the Fund for Scientific Research-Flanders (FWO grant G.0022.08) and the Research Council of Ghent University (projects BOF2005/GOA/008 and BOF2007/GOA/0017). The authors want to thank The Consortium for Functional Glycomics funded by the NIGMS GM62116 for the glycan array analysis.

## References

1. Peumans, W.J., Van Damme, E.J.M.: Lectins as plant defense proteins. *Plant Physiol.* **109**, 347–352 (1995)
2. Van Damme, E.J.M., Lannoo, N., Peumans, W.J.: Plant lectins. *Adv. Bot. Res.* **48**, 107–209 (2009)
3. Lannoo, N., Van Damme, E.J.M.: Nucleocytoplasmic plant lectins. *Biochem. Biophys. Acta* **1800**, 190–201 (2009)
4. Rini, J.M.: Lectin structure. *Annu. Rev. Biophys. Biomol. Struct.* **24**, 551–577 (1995)
5. Sinha, S., Gupta, G., Vijayan, M., Surolia, A.: Subunit assembly of plant lectins. *Curr. Opin. Struct. Biol.* **17**, 498–505 (2007)
6. Chen, Y., Peumans, W.J., Hause, B., Bras, J., Kumar, M., Proost, P., Barre, A., Rougé, P., Van Damme, E.J.M.: Jasmonate methyl ester induces the synthesis of a cytoplasmic/nuclear chito-oligosaccharide-binding lectin in tobacco leaves. *FASEB J.* **16**, 905–907 (2002)
7. Lannoo, N., Peumans, W.J., Van Damme, E.J.M.: Do F-box proteins with a C-terminal domain homologous with the tobacco lectin play a role in protein degradation in plants? *Biochem. Soc. Trans.* **36**, 843–847 (2008)
8. Dinant, S., Clark, A.M., Zhu, Y.M., Vilaine, F., Palauqui, J.C., Kusiak, C., Thompson, G.A.: Diversity of the superfamily of phloem lectins (Phloem protein 2) in angiosperms. *Plant Physiol.* **131**, 114–128 (2003)
9. Lannoo, N., Peumans, W.J., Van Pamel, E., Alvarez, R., Xiong, T. C., Hause, G., Mazars, C., Van Damme, E.J.M.: Localization and *in vitro* binding studies suggest that the cytoplasmic/nuclear tobacco lectin can interact *in situ* with high mannose and complex N-glycans. *FEBS Lett.* **580**, 6329–6337 (2006)
10. Lannoo, N., Vandenborre, G., Miersch, O., Smagghe, G., Wasternack, C., Peumans, W.J., Van Damme, E.J.M.: The jasmonate-induced expression of the *Nicotiana tabacum* leaf lectin. *Plant Cell Physiol.* **48**, 1207–1218 (2007)
11. Vandenborre, G., Miersch, O., Hause, B., Smagghe, G., Wasternack, C., Van Damme, E.J.M.: *Spodoptera littoralis* induced lectin expression in tobacco. *Plant Cell Physiol.* **50**, 1142–1155 (2009)
12. Lannoo, N., Vervecken, W., Proost, P., Rougé, P., Van Damme, E. J.M.: Expression of the nucleocytoplasmic tobacco lectin in the yeast *Pichia pastoris*. *Protein Expr. Purif.* **53**, 275–282 (2007)
13. Thompson, J.D., Gibson, T.J., Plewniak, F., Jeanmougin, F., Higgins, D.G.: The CLUSTAL-X windows interface: flexible strategies for multiple sequence alignment aided by quality analysis tools. *Nucleic Acids Res.* **25**, 4876–4882 (1997)

14. Risler, J.L., Delorme, M.O., Delacroix, H., Henaut, A.: Amino acid substitutions in structurally related proteins—a pattern-recognition approach—determination of a new and efficient scoring matrix. *J. Mol. Biol.* **204**, 1019–1029 (1988)
15. Gaboriaud, C., Bissery, V., Benchetrit, T., Mornon, J.-P.: Hydrophobic cluster analysis: an efficient new way to compare and analyse amino acid sequences. *FEBS Lett.* **224**, 149–155 (1987)
16. Xie, H.F., Gilbert, H.J., Charnock, S.J., Davies, G.J., Williamson, M.P., Simpson, P.J., Raghothama, S., Fontes, C.M.G.A., Dias, F. M.V., Ferreira, L.M.A., Bolam, D.N.: *Clostridium thermocellum* Xyn10B carbohydrate-binding module 22-2: the role of conserved amino acids in ligand binding. *Biochemistry* **40**, 9167–9176 (2001)
17. Ponder, J.W., Richards, F.M.: Tertiary templates for proteins—use of packing criteria in the enumeration of allowed sequences for different structural classes. *J. Mol. Biol.* **193**, 775–779 (1987)
18. Mas, M.T., Smith, K.C., Yarmush, D.L., Aisaka, K., Fine, R.M.: Modeling the anti-CEA antibody combining site by homology and conformational search. *Protein Struct. Funct. Genet.* **14**, 483–498 (1992)
19. Laskowski, R.A., Macarthur, M.W., Moss, D.S., Thornton, J.M.: Procheck—a program to check the stereochemical quality of protein structures. *J. Appl. Crystallogr.* **26**, 283–291 (1993)
20. Nicholls, A., Sharp, K.A., Honig, B.: Protein folding and association—insights from the interfacial and thermodynamic properties of hydrocarbons. *Protein Struct. Funct. Genet.* **11**, 281–296 (1991)
21. Gilson, M.K., Honig, B.H.: Calculation of electrostatic potential in an enzyme active site. *Nature* **330**, 84–86 (1987)
22. Blixt, O., Head, S., Mondala, T., Scanlan, C., Alvarez, R., Bryan, M.C., Fazio, F., Calarese, D., Stevens, J., Razi, N., van Die, I., Burton, D., Wilson, I.A., Cummings, R., Huflejt, M.E., Bovin, N., Wong, C.H., Paulson, J.C.: Printed covalent glycan array for ligand profiling of diverse glycan binding proteins. *Proc. Natl. Acad. Sci. U.S.A.* **101**, 17033–17038 (2004)
23. Bradford, M.M.: Rapid and sensitive method for quantitation of microgram quantities of protein utilizing principle of protein-dye binding. *Anal. Biochem.* **72**, 248–254 (1976)
24. Laemmli, U.K.: Cleavage of structural proteins during assembly of head of bacteriophage T4. *Nature* **227**, 680–685 (1970)
25. Gomez, G., Torres, H., Pallas, V.: Identification of translocatable RNA-binding phloem proteins from melon, potential components of the long distance RNA transport system. *Plant J.* **41**, 107–116 (2005)
26. Anantharam, V., Patanjali, S.R., Surolia, A.: A chitotetrose specific lectin from *Luffa acutangula*—physicochemical properties and the assignment of orientation of sugars in the lectin binding site. *J. Biosci.* **8**, 403–411 (1985)
27. Anantharam, V., Patanjali, S.R., Swamy, M.J., Sanadi, A.R., Goldstein, I.J., Surolia, A.: Isolation, macromolecular properties, and combining site of a chitooligosaccharide-specific lectin from the exudate of ridge gourd (*Luffa acutangula*). *J. Biol. Chem.* **261**, 4621–4627 (1986)
28. Sanadi, A.R., Anantharam, V., Surolia, A.: Elucidation of the combining site of *Coccinia indica* agglutinin (CIA) by thermodynamic analyses of its ligand binding. *Pure Appl. Chem.* **70**, 677–686 (1998)
29. Narahari, A., Swamy, M.J.: Tryptophan exposure and accessibility in the chitooligosaccharide-specific phloem exudate lectin from pumpkin (*Cucurbita maxima*). A fluorescence study. *J. Photochem. Photobiol. B* **97**, 40–47 (2009)